Theory of Magnetic Breakdown, g Factor, and Energy-Band Structure of Zinc*†

J. P. VAN DYKE,‡ J. W. MCCLURE, AND J. F. DOAR
Department of Physics, University of Oregon, Eugene, Oregon 97403
(Received 1 December 1969)

The Landau levels associated with the "needle" in zinc have been studied by numerically solving the coupled differential equations given by applying the method of Luttinger and Kohn to Bennett and Falicov's $\mathbf{k}\cdot\mathbf{p}$ model. The "leakage" probability amplitudes and phases for tunneling from one monster through the needle to another monster agree with Pippard's semiclassical calculation. Thus, the Pippard network model and the magnetoresistance theory of Falicov, Pippard, and Sievert is justified. There is still some question as to the effect of magnetic breakdown on the de Haas–van Alphen amplitude associated with the needle. Because of the complicated Landau level structure, which comes from the near degeneracy of the bands, the various possible definitions of the g factor do not agree. The data from the magnetoresistance, the de Haas–van Alphen effect, and the de Haas–van Alphen effect under pressure have been used to find two possible sets of energy-band parameters for the needle. Using a plausible definition of the g factor, the band parameter solution which agrees most closely with other theoretical calculations corresponds to a g factor of 170, while the other solution corresponds to $g=-170$. An experimental selection of the correct solution would be provided by a measurement of the effect of pressure upon the breakdown field. The changes in the de Haas–van Alphen period and effective mass with alloying can be accounted for by reasonable changes in band parameters, but the predicted change in breakdown field is very different from the experimental results of Higgins and Marcus.

I. INTRODUCTION

SEVERAL goals led to the present investigation of the structure of the Landau levels associated with the "needle" in zinc: (1) to understand the spin splitting of the levels, (2) to test the semiclassical theory of magnetic breakdown, (3) to determine the energy-band structure near the needle, and (4) to explain the effects of pressure and alloying upon the de Haas–van Alphen effect. It was further desired to use a single method of calculation that would yield all the relevant features of the Landau levels.

The spin splitting of the needle Landau levels is large and is resolved in oscillations of the magnetoresistance[1] as a function of magnetic field and in the de Haas–van Alphen effect.[2] Stark[1] showed that his data were consistent with g factors of ± 90, ± 180, or ± 360. Bennett and Falicov[3] used a three-band $\mathbf{k}\cdot\mathbf{p}$ model to calculate the g factor, and found an upper limit of $g=266$ (including the correction of a factor 2 error in the original paper). However, their calculation used a perturbation theory which is valid only if the Fermi level is very close to the needle band edge, a condition which we shall see is not met in zinc. O'Sullivan and Schirber[2] argued from a combination of their experimental de Haas–van Alphen data and a simple theoretical model that the absolute magnitude of the g factor is equal to 170. We shall see below that owing to the complexity of the Landau-level structure, different definitions of the g factor can give different values.

The concept of magnetic breakdown was first proposed by Cohen and Falicov[4] in 1961. At first approximate[5–8] and then more exact[9,10] treatments showed that the tunneling probability can be expressed as $p^2=e^{-H_0/H}$, where the breakdown field H_0 is a specified function of the energy-band parameters. Pippard[7,11] introduced a semiclassical method for calculating the energy levels of a network of free-electron orbits coupled by magnetic breakdown. He obtained numerical results for the energy levels of an infinite hexagonal network[11] which could represent zinc or magnesium. He then Fourier analyzed the density of states to find the effect upon the amplitude of the de Haas–van Alphen effect. He found that the amplitude is proportional to q^3 for large needles and to $q^{3.6}$ for the needle size in magnesium, where $q^2=1-p^2$. The needles in zinc are smaller than those in magnesium. Falicov and Stachowiak[12] developed a Green's function theory for the magnetic susceptibility of a network and found that the de Haas–van Alphen amplitude of the needle is always proportional to q^3. Higgins and Marcus[13] used the q^3 rule to analyze their de Haas–van Alphen results

* Research supported by the National Science Foundation.
† Paper based in part on a thesis submitted by one of the authors (J. P. Van Dyke) in partial fulfillment of the requirements for the Ph.D. degree at the University of Oregon.
‡ Present address: Sandia Laboratory, Albuquerque, N. M. 87115.
[1] R. W. Stark, Phys. Rev. **135**, A1698 (1964).
[2] W. J. O'Sullivan and J. E. Schirber, Phys. Rev. **162**, 519 (1967).
[3] A. J. Bennett and L. M. Falicov, Phys. Rev. **136**, A998 (1964).
[4] M. H. Cohen and L. M. Falicov, Phys. Rev. Letters **7**, 231 (1961). For a review of magnetic breakdown, see R. W. Stark and L. M. Falicov, *Progress in Low-Temperature Physics* (North-Holland Publishing Co., Amsterdam, 1967), Vol. 5, p. 235.
[5] E. I. Blount, Phys. Rev. **126**, 1636 (1962).
[6] W. A. Harrison, Phys. Rev. **126**, 497 (1962).
[7] A. B. Pippard, Proc. Roy. Soc. (London) **A270**, 1 (1962).
[8] J. R. Reitz, J. Phys. Chem. Solids **25**, 53 (1964).
[9] U. N. Upadyaya, Bull. Am. Phys. Soc. **9**, 635 (1964); Office of Naval Research, Project NR 017-633, Technical Report No. 4 (unpublished).
[10] C. B. Duke and W. A. Harrison (private communication). These authors and Upadyaya (Ref. 9) made exact solutions of Blount's effective Hamiltonian (Ref. 5). The mathematics is the same as for another problem solved by C. Zener, Proc. Roy. Soc. (London) **A137**, 696 (1932).
[11] A. B. Pippard, Phil. Trans. Roy. Soc. London **A256**, 317 (1964).
[12] L. M. Falicov and H. Stachowiak, Phys. Rev. **147**, 505 (1966).
[13] R. J. Higgins and J. A. Marcus, Phys. Rev. **161**, 589 (1967).

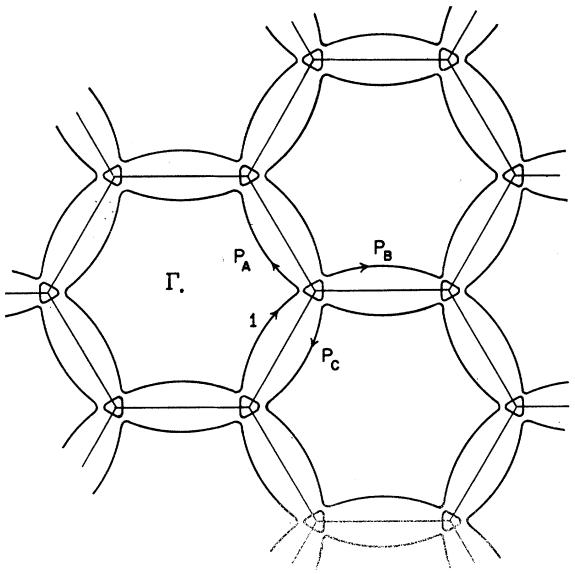

FIG. 1. Fermi-surface cross section in zinc in the plane $k_z=0$, z parallel to the hexad axis. The hexagons are Brillouin-zone cross sections and the hexagon corners are the symmetry points K. The small triangular shapes are cross sections of the needle, magnified by about a factor of 10. The larger starlike shapes are cross sections of the monster. The labels P_A etc. illustrate the definition of the leakage probabilities.

and found $H_0=2.2\pm0.1$ kG. The semiclassical network theory has been tested for a *finite* network model which can be solved exactly.[14,15] It was found that the Pippard theory gives good agreement for the spacings of the energy levels[14] and that the Falicov-Stachowiak theory gives good results for the amplitudes of the de Haas–van Alphen effect.[15] The present calculation justifies the use of the basic semiclassical network model for zinc, but does not resolve the discrepancy in the de Haas–van Alphen amplitude factor.

The magnetoresistance of zinc is strikingly affected by magnetic breakdown.[1] Falicov, Pippard, and Sievert[16] made a theory of the magnetoresistance using the network model. Their theory could explain Stark's[1] experiments when the breakdown field was chosen to be $H_0=2.7$ kG. Chambers[17] has justified the use of the network model for the magnetoresistance by a direct calculation very similar to the one presented here.

In the present paper we use the experimental information from the de Haas–van Alphen effect and the magnetoresistance to determine the energy band structure near the needle. Previously, this information has been only partially used. The de Haas–van Alphen periods for various parts of the Fermi surface have been used with the few-orthogonalized-plane-waves (OPW) model[6] and with a nonlocal-pseudopotential model[18] to determine the energy-band structure throughout the entire Brillouin zone. Bennett and Falicov[3] used the effective mass and spin splitting to determine some of the parameters in their model. We shall make use of the de Haas–van Alphen and Shubnikov–de Haas period, effective mass, spin splitting, breakdown field, and pressure dependence of the first three quantities to determine the parameters in the Bennett-Falicov model for the needle.

Several experimental studies have been made of the effect of pressure upon the de Haas–van Alphen effect in zinc.[2,19,20] The Bennett-Falicov model is adapted to zinc under pressure by changing the values of some of the parameters. As mentioned above, the pressure dependence of the experimental quantities is used to help determine the band parameters. Experimental studies have also been made of the effect of alloying upon the de Haas–van Alphen effect in zinc.[13,21,22] We try to account for the effects of alloying by changing the values of the same band parameters which were allowed to change with pressure. Though we can account for the changes in the period and effective mass in a reasonable fashion, it is not possible to account for the change in breakdown field. The last result is in agreement with a qualitative argument by Higgins and Marcus.[13]

The band model and method of calculation is explained in Sec. II. The general features of the results are discussed and compared with the semiclassical theory in Sec. III. The question of the value of the g factor is also discussed in Sec. III. The experimental data are used to determine the band parameters and the results compared to theoretical predictions in Sec. IV. The effects of alloying are discussed in Sec. V and the conclusions are summarized in Sec. VI.

II. ENERGY-BAND MODEL AND METHOD OF CALCULATION

The Brillouin zone of zinc is a hexagonal cylinder. Energy band calculations by the OPW method,[6] the pseudopotential method,[18] and the augmented-plane-wave method[23] all give results fairly near the free-electron band structure. Figure 1 shows a cross section of part of the Fermi surface in the plane $k_z=0$ (z parallel to the hexad axis). The small triangular pieces near the zone corners K are the needles, so-called be-

[14] J. Ruvalds and J. W. McClure, J. Phys. Chem. Solids **28**, 509 (1967).
[15] J. Ruvalds, J. Phys. Chem. Solids **30**, 305 (1969).
[16] L. M. Falicov, A. B. Pippard, and P. R. Sievert, Phys. Rev. **151**, 498 (1967).
[17] W. G. Chambers, J. Phys. C **1**, 1608 (1968).
[18] R. W. Stark and L. M. Falicov, Phys. Rev. Letters **19**, 795 (1967); and unpublished.
[19] See W. J. O'Sullivan and J. E. Schirber, Phys. Rev. **151**, 484 (1966) and references cited therein; P. J. Melz, Ph.D. thesis, University of Illinois, 1966 (unpublished).
[20] E. S. Itskevich, A. N. Vosnovskii, and V. A. Sukhoparov, Zh. Eksperim. i Teor. Fiz. Pis'ma v Redaktsiyu **2**, 67 (1965) [English transl.: Soviet Phys.—JETP Letters **2**, 42 (1965)].
[21] R. J. Higgins and J. A. Marcus, Phys. Rev. **141**, 553 (1966).
[22] J. R. Lawson and W. L. Gordon, Bull. Am. Phys. Soc. **14**, 402 (1969); and unpublished; J. R. Lawson, Ph.D. thesis, Case Western Reserve University, 1969 (unpublished).
[23] L. F. Matheiss, Phys. Rev. **134**, A970 (1964).

cause the surfaces are long in the z direction. The larger pieces are part of the monster. We are concerned with the Landau levels associated with the needles when the magnetic field H is parallel to the hexad axis. The levels are modified by magnetic breakdown between the needle and the monster. The semiclassical orbits in k space are the curves of constant energy shown in Fig. 1. The orbits in direct space have the same shape but are rotated 90° (even the small needle orbit in direct space includes many unit cells of the lattice). The Pippard treatment[7,11] replaces the orbits in direct space by a set of intersecting circles. The electron is considered to travel on the circle, with a probability of changing circles at a junction. To treat the magnetoresistance, Falicov, Pippard, and Sievert[16] calculated the "leakage" probabilities for an electron incident on one of the input channels (labeled 1 in Fig. 1) to exit on each of the three output channels (labeled P_A, P_B, and P_C in Fig. 1). Resonance on the needle causes these probabilities to be modulated with the de Haas–van Alphen frequency.

Two aspects of the semiclassical treatment seem likely to produce errors: (1) the distortion of the true orbits into intersecting circles and (2) the neglect of the width of the orbit, which is approximately $S^{-1/2}$, where $S=eH/\hbar c$. For example, when a low quantum number Landau level is at the Fermi level, the size of the needle orbit in direct space is about $S^{-1/2}$. Both of these effects are important only near the needle.

Our procedure is to apply the method of Luttinger and Kohn[24] to the $\mathbf{k}\cdot\mathbf{p}$ model of Bennett and Falicov,[3] yielding a set of coupled differential equations. The equations are then solved numerically with the boundary conditions that the solutions match onto the Pippard solutions far from the needle.

The $\mathbf{k}\cdot\mathbf{p}$ model is a Taylor expansion of the one-electron Hamiltonian about the symmetry point K. As the average radius of the needle in inverse atomic units is about 0.006, and that of the Brillouin zone is about 0.8, only the lowest-order terms in k need be kept. Near the point K there are three pairs of doubly degenerate bands with energies near the Fermi level, of symmetry types[3] K_7, K_8, and K_9. The energy differences of importance for these bands are all less than 0.01 Ry, while the nearest other bands at K lie about 0.4 Ry away.[23] Thus, only the six-band sub-Hamiltonian need be considered. Furthermore, the sub-Hamiltonian does not mix spin up and spin down so that one can treat two three-band sub-Hamiltonians. With these approximations, Bennett and Falicov[3] have shown that the most general sub-Hamiltonian allowed by symmetry is

$$\mathcal{H}=\begin{bmatrix} 0 & (A+\sigma C)\hbar k_- & (A-\sigma C)\hbar k_+ \\ (A+\sigma C)\hbar k_+ & E_c+\sigma\Delta/3 & B\hbar k_- \\ (A-\sigma C)\hbar k_- & B\hbar k_+ & E_c-\sigma\Delta/3 \end{bmatrix}, \quad (2.1)$$

where $\sigma=+1$ for spin up and -1 for spin down, the order of basis states is K_7, K_8, K_9 for spin up and K_7, K_9, K_8 for spin down, energy is measured from the K_7 level, the origin of k is the point K, and $k_\pm$ is defined by $k_\pm=k_x\pm ik_y$. The quantity E_c is the crystal potential gap (called E by Bennett and Falicov) which would be the K_1, K_5 splitting in the absence of spin-orbit coupling ($K_7\rightarrow K_1$; K_8, $K_9\rightarrow K_5$). Harrison[6] and Mattheiss[23] found E_c to be negative, but smaller than the estimated error of calculation, while Stark and Falicov[18] found $E_c=0.0035$ Ry. The quantity Δ is the spin-orbit constant which Bennett and Falicov[3] estimated as 0.004 or 0.008 Ry and for which Stark and Falicov[18] found 0.0075 Ry. The quantities A, B, and C are velocity matrix elements. For nearly free electrons, one has $A=B=\hbar k_c/m_0\equiv A_F$, where k_c is the magnitude of the wavevector from the zone center Γ to the corner K. In atomic units, $A_F=0.835$. The quantity C is the spin-orbit part of the velocity matrix element. Its magnitude was estimated by Bennett and Falicov[3] as $C=\Delta/6m_0A$. Our numerical calculations show that changing C from the above value to zero has an effect upon the experimental quantities which is less than half the experimental error. Thus, we neglect C in the rest of the paper, but the details of calculations including C can be found in the thesis of one of the authors.[25]

A final parameter, which does not appear in the sub-Hamiltonian (2.1), is the energy of the Fermi level, which we call ζ when it is measured from the K_7 level and μ when it is measured from the needle band edge. If $E_c<-\frac{1}{3}\Delta$, the needle band edge is the K_7 level and $\mu=\zeta$, while if $E_c>-\Delta/3$, the needle band edge is the K_8 level (for spin up) and $\mu=\zeta-E_c-\Delta/3$.

The sub-Hamiltonian may be diagonalized numerically to find the energy-band structure in the neighborhood of point K. Figure 2 shows the energy as a function of k_x and Fig. 3 shows the cross section of the needle, both curves being calculated for one of the possible sets of band parameters of zinc. The effective Hamiltonian used by Chambers[17] is equivlaent to (2.1) with $C=0$ and $A=B=A_F$, though it is given in a different representation and with a coordinate system rotated 90° from ours.

To introduce the magnetic field,[26] we choose the Landau gauge for the vector potential $\mathbf{A}=(0,H_x,0)$ and use the prescription of Luttinger and Kohn[24]: k_y is

[24] J. M. Luttinger and W. Kohn, Phys. Rev. **97**, 869 (1955).

[25] J. P. Van Dyke, Ph.D. thesis, University of Oregon, 1967 (unpublished) (No. 67-10, 791, available from University Microfilm Corporation, Ann Arbor, Mich. 48106).

[26] We may use the method of Luttinger and Kohn because we need solutions over only a small part of the Brillouin zone. For methods valid over the entire Brillouin zone, see W. G. Chambers (Ref. 29) and E. Brown, in *Solid-State Physics*, edited by F. Seitz and D. Turnbull (Academic Press Inc., New York, 1968), Vol. 22, p. 213. Numerical calculations for another infinite network are in F. A. Butler and E. Brown, Phys. Rev. **166**, 630 (1968). Very interesting calculations over the full zone for a single-band model of zinc have been performed by P. S. Kapo, Ph.D. thesis, Rensselaer Polytechnic Institute, 1967 (unpublished).

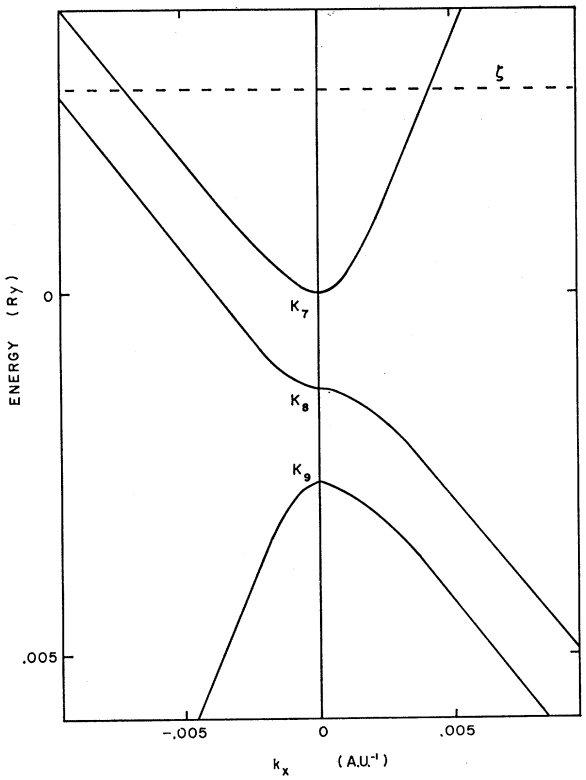

FIG. 2. Energy versus wave number in the x direction (Γ–K line) around point K. The figure is drawn to scale for case 2, one of the two possible sets of band parameters for zinc (see Table I). The distance from Γ to K is 0.835 in a.u.$^{-1}$ The Fermi level is indicated by the dashed line.

replaced by $k_y - iS\partial/\partial k_x$. The Schrödinger equation $\mathcal{H}\psi = E\psi$ now becomes a set of three coupled first-order differential equations in k space. To complete the system, boundary conditions must be specified. However, we defer the discussion of the boundary conditions until after a discussion of the properties of the solutions.

If we write each component of the three-component wave function as

$$\psi_i(k_x,k_y) = \exp[-ik_xk_y/S]g(k_y)f_i(k_x), \qquad (2.2)$$

where $g(k_y)$ is an arbitrary function, the equations for the f_i are the same as the equations for the ψ_i except that $k_y - iS\partial/\partial k_x$ becomes simply $-iSd/dk_x$ and $k_\pm$ in (2.1) becomes $k_x \pm Sd/dk_x$. We further introduce the change of variables $u = 2A\hbar k_x/\Delta$ and

$$s = 2S\hbar^2 A(2A^2+B^2)^{1/2}/\Delta^2,$$

and make the transformation $\mathcal{H}' = U^{-1}\mathcal{H}U$, $Y = U^{-1}f$, where

$$U = \begin{bmatrix} 0 & -2^{1/2}A/(2A^2+B^2)^{1/2} & B/(2A^2+B^2)^{1/2} \\ -2^{1/2} & B/(2A^2+B^2)^{1/2}2^{1/2} & A/(2A^2+B^2)^{1/2} \\ 2^{1/2} & B/(2A^2+B^2)^{1/2}2^{1/2} & A/(2A^2+B^2)^{1/2} \end{bmatrix}. \qquad (2.3)$$

The transformed system of equations is

$$-sdY_2/du = (P_1u+D_1)Y_1 + D_6Y_2 + D_5Y_3, \qquad (2.4a)$$

$$sdY_1/du = D_6Y_1 + (P_2u+D_2)Y_2 + (P_4u+D_4)Y_3, \qquad (2.4b)$$

$$0 = D_5Y_1 + (P_4u+D_4)Y_2 + (P_3u+D_3)Y_3, \qquad (2.4c)$$

where

$$P_1 = -B/2A, \qquad (2.5a)$$

$$P_2 = -\tfrac{1}{2}(B/A)(4A^2-B^2)/(2A^2+B^2), \qquad (2.5b)$$

$$P_3 = 3AB/(2A^2+B^2), \qquad (2.5c)$$

$$P_4 = 2^{1/2}(B^2-A^2)/(2A^2+B^2), \qquad (2.5d)$$

$$D_1 = \xi - \epsilon, \qquad (2.5e)$$

$$D_2 = [\xi B^2/(2A^2+B^2)] - \epsilon, \qquad (2.5f)$$

$$D_3 = [2\xi A^2/(2A^2+B^2)] - \epsilon, \qquad (2.5g)$$

$$D_4 = 2^{1/2}\xi AB/(2A^2+B^2), \qquad (2.5h)$$

$$D_5 = -2^{1/2}\sigma A/3(2A^2+B^2)^{1/2}, \qquad (2.5i)$$

$$D_6 = -\sigma B/3(2A^2+B^2)^{1/2}, \qquad (2.5j)$$

and $\epsilon \equiv \zeta/\Delta$ and $\xi \equiv E_c/\Delta$.

It is remarkable that use of the particular Landau gauge plus the transformation has reduced the system to two coupled differential equations, thus saving computer time. We shall see below that there are still three independent solutions. We can transform the system into a single second-order differential equation; further, it can be put into the form of a one-dimensional Schrödinger equation with an effective potential[25] which has an attractive well, corresponding to the needle, separated by barriers from a region in which the potential function is less than inside the well. Treatment of this equation by the WKB approximation[25] yields the Onsager-Lifshitz area-quantization rules[27] for de Haas–van Alphen period and effective mass, the semiclassical tunneling probability[5–10]; and, when treated to next order in S, an expression for the g factor.

For the exact treatment, we used Eq. (2.4c) to eliminate Y_3, and numerically solved the two coupled linear differential equations for Y_1 and Y_2. The numerical integrations were started near $u = U_p \equiv -D_3/P_3$, which corresponds to the right-hand side of the needle shown in Fig. 3.

Defining $z = u - U_p$, three real independent solutions near this point may be written

$$Y_1^A = P_4U_p + D_4 + O(z), \qquad (2.6a)$$

$$Y_2^A = -D_5 + O(z), \qquad (2.6b)$$

$$Y_3^A = O(1), \qquad (2.6c)$$

[27] L. Onsager, Phil. Mag. **43**, 1006 (1952); I. M. Lifshitz in notes added in proof to D. Shoenberg, *Progress in Low-Temperature Physics* (North-Holland Publishing Co., Amsterdam, 1957), Vol. 2, p. 226.

$$Y_1{}^L = Y_1{}^A \ln|z| + O(z), \tag{2.7a}$$

$$Y_2{}^L = Y_2{}^A \ln|z| - [sP_3/(P_4U_p + D_4)] + O(z), \tag{2.7b}$$

$$Y_3{}^L = Y_3{}^A \ln|z| + (s/z) + O(1), \tag{2.7c}$$

$$Y_1{}^D = \theta(z) Y_1{}^A, \tag{2.8a}$$

$$Y_2{}^D = \theta(z) Y_2{}^A, \tag{2.8b}$$

$$Y_3{}^D = 2s\delta(z) + \theta(z) Y_3{}^A, \tag{2.8c}$$

where $\theta(z)$ is the Heaviside step function $\theta(z)=1$, $z>0$; $\theta(z)=-1$, $z<0$. The superscripts A, L, and D stand for analytic, logarithmic, and delta-function solutions. The solution D, which involves discontinuities and the delta function, is a solution to Eqs. (2.4) but is not a solution of the system of equations obtained by eliminating Y_3. Starting with these forms, solutions for Y^A and Y^L were found for positive and negative z by using the fourth-order Runge-Kutta method on an IBM 360/50. The Wronskian of the two solutions is constant, $Y_1{}^A Y_2{}^L - Y_1{}^L Y_2{}^A = -P_3 s$. Once Y^A is known, Y^D is also known.

For large values of $|u|$, any real solution can be written in the asymptotic form

$$Y_1 \sim A_m[(2A^2+B^2)/3B^2]^{1/4} \cos[\varphi(u) + \delta\varphi], \tag{2.9a}$$

$$Y_2 \sim A_m[3B^2/(2A^2+B^2)]^{1/4} \sin[\varphi(u) + \delta\varphi], \tag{2.9b}$$

$$Y_3 \sim -(P_4/P_3) Y_2, \tag{2.9c}$$

where the phase function $\varphi(u)$ is

$$\varphi(u) = [(2A^2+B^2)^{1/2}/4s\sqrt{3}] \times [u^2 + 4U_p u + O(u^{-1})], \tag{2.9d}$$

and $\delta\varphi$ is a constant phase shift. These forms become exact solutions in the trival case $A=B$, $E_c=\Delta=0$. Our computer program integrates the equations until the numerical solutions match the asymptotic form (2.9) with suitably chosen amplitude A_m and phase $\delta\varphi$. The typical total range of numerical integration was about one-tenth of the diameter of the Brillouin zone.

The physical significance of the limiting solutions is best exhibited by transforming to direct space and symmetric gauge. The transformed wave function is[24]

$$\Psi(\mathbf{r}) = \sum_i u_i(\mathbf{r}) \chi_i(x,y), \tag{2.10a}$$

$$\chi_i(x,y) = \exp[-iSxy] \int dk_x \int dk_y \times \exp[i(k_x x + k_y y)] \psi_i(k_x, k_y), \tag{2.10b}$$

where u_i is the Bloch wave at K associated with Y_i. In order for the wave functions far from possible tunnelling points (junctions) to match smoothly onto Pippard's free-electron functions, we must chose the function g in Eq. (2.2) to be of the form $g(k_y) = \exp(-k_y{}^2/2S)$. With this choice, the part of χ_3 contributed by the delta function in the solution

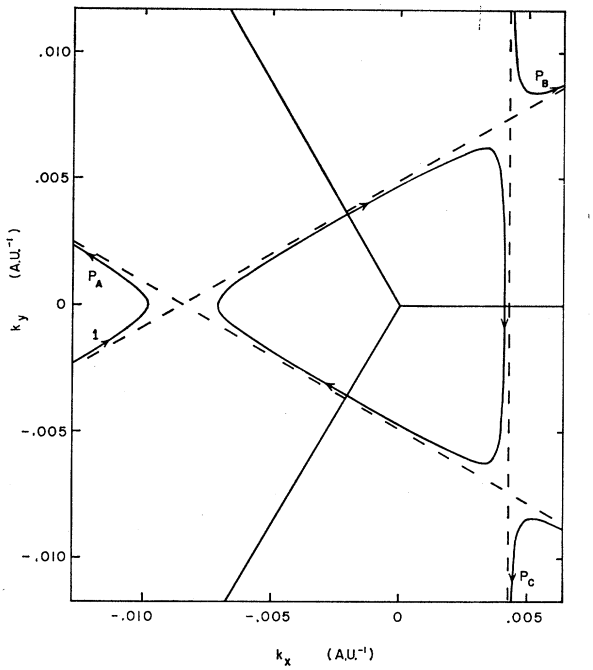

FIG. 3. Cross section of the needle Fermi surface. The figure is drawn to scale for case 2, one of the two possible sets of band parameters for zinc (see Table I). The labels P_A, etc., are related to the definition of the leakage probabilities.

(2.8c) is

$$\chi_3' = (2\pi S)^{1/2} (\Delta s/2A\hbar) \mu(x,y), \tag{2.11a}$$

$$\mu(x,y) = \exp\tfrac{1}{2}[-S(y - k_0/S)^2 + ik_0 x - i(y - k_0/S)Sx], \tag{2.11b}$$

where $k_0 = \Delta U_p/2A\hbar$ is the distance from the center of the needle to its right-hand edge. The function (2.11) describes an electron moving in the positive x direction along a "track" of width about $S^{-1/2}$ centered at $y = k_0/S$. This corresponds to the vertical asymptotes shown in Fig. 3, and we call it channel 1. The contribution to a χ_i from a Y_i equal to $\exp[i\varphi(u)]$ is

$$\chi_i'' = \pi S(2\sqrt{3})^{1/2} \times \exp i[(\pi/12) - k_0{}^2/2\sqrt{3}S] \mu(x',y'), \tag{2.12}$$

where $x' = -\frac{1}{2}x + \frac{1}{2}\sqrt{3}y$, $y' = -\frac{1}{2}y - \frac{1}{2}\sqrt{3}x$. This function represents an electron traveling along an orbit rotated by $2\pi/3$ from the orbit just discussed, and we call it channel 3. The contribution from a Y_i equal to $\exp[-i\varphi(u)]$ is the same as (2.12) except that the sign of the phase factor $\exp i[(\pi/12) - k_0{}^2/2\sqrt{3}S]$ is changed and the orbit is rotated by $-2\pi/3$ from the first orbit. This last orbit we call channel 2. These functions are valid for distances from the origin much greater than k_0/S (the size of the needle in direct space) but much less than k_c/S (the size of the monster). Thus, our asymptotic functions serve to match Pippard's wave functions far from the junction to our numerical solutions.

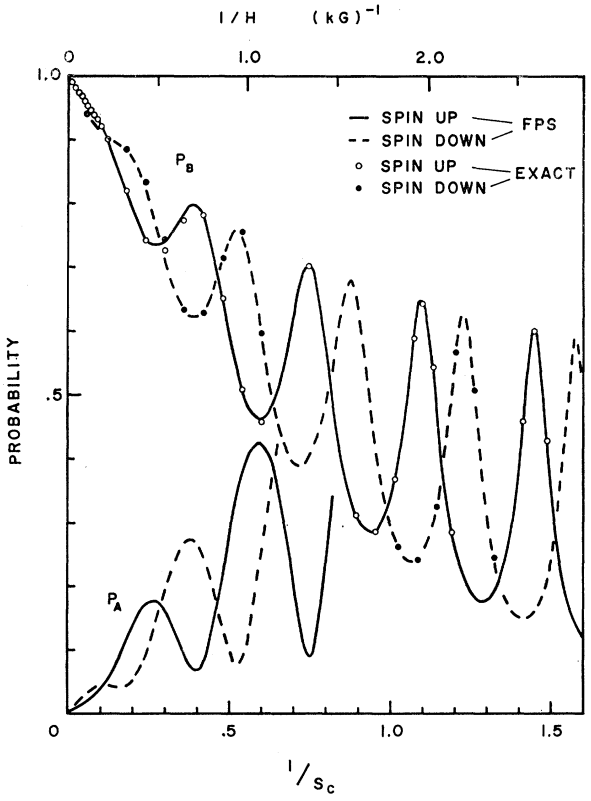

FIG. 4. The leakage probabilities as a function of inverse magnetic field strength. The circles are the results of the exact numerical calculations and the lines are the semiclassical theory with the period and phases adjusted to give best agreement with the exact results. The results are for case 3, one of the two possible sets of band parameters for zinc (see Table I). The abscissa is related to the quantity used in the text by $S_c=1.098s$.

In order to use the trigonal symmetry, we change to the same basis functions used by Chambers[17]: $|k_1\rangle$, $|k_2\rangle$, $|k_3\rangle$, where $|k_1\rangle$ rotated by $2\pi/3$ becomes $|k_3\rangle$, etc. In the free-electron case, $|k_1\rangle$ is just the plane wave with $\mathbf{k}=(k_c,0,0)$. The relation to the basis states K_7, K_8, K_9 are[3] (for spin up)

$$|K_7\rangle=|k_1\rangle+\omega^2|k_2\rangle+\omega|k_3\rangle, \tag{2.13a}$$

$$|K_8\rangle=|k_1\rangle+|k_2\rangle+|k_3\rangle, \tag{2.13b}$$

$$|K_9\rangle=|k_1\rangle+\omega|k_2\rangle+\omega^2|k_3\rangle, \tag{2.13c}$$

where $\omega=\exp(2\pi i/3)$. In terms of these basis functions, the part of an asymptotic solution such as (2.9) going like $\exp(i\varphi)$ becomes

$$i\omega A_m\pi S(\sqrt{3}/2)^{1/2}\exp i[\delta\varphi+(\pi/12)-k_0^2/2\sqrt{3}S] \times\mu(x',y')[\omega^2\beta|k_1\rangle+\omega\beta|k_2\rangle+\alpha|k_3\rangle], \tag{2.14}$$

where $\alpha=(2A+B)/[3(2A^2+B^2)]^{1/2}$ and $\beta=(B-A)/[3(2A^2+B^2)]^{1/2}$. The phase factor $i\omega\exp i[\delta\varphi+(\pi/12)-k_0^2/2\sqrt{3}S]$ can be written $\exp i[\delta\varphi+(5\pi/4)-k_0^2/2\sqrt{3}S]=\exp i\tau$. To obtain the contribution from the $\exp(-i\varphi)$ factor, we take the complex conjugate of the phase factor and rotate the rest of the function by $+2\pi/3$.

To make contact with Pippard's work, we want to find the probability amplitudes for the three output channels (labeled P_A, P_B, and P_C in Figs. 1 and 3) when a wave of unit intensity is on one of the input channels. We can satisfy the conditions on the input channels by taking the correct linear combination of three independent solutions. The easiest three solutions to use are the analytic solution (which contains only channels 2 and 3) and the functions obtained by $\pm2\pi/3$ rotations of the analytic solution. Calling $\delta\varphi_{L,R}$ the phase shift on the left or right side for the analytic solution and $A_{L,R}$ the corresponding amplitude factor, we find for the probability amplitudes

$$a=[(A_L^2-A_R^2)/A_Rd]\exp[i(\delta\varphi_R+\tau)], \tag{2.15a}$$

$$b=\{A_R\exp[-i(\delta\varphi_R+2\delta\varphi_L+3\tau)] +A_L\exp[i(2\delta\varphi_R+\delta\varphi_L+3\tau)]\}/d, \tag{2.15b}$$

$$c=[(A_R^2-A_L^2)/A_Ld]\exp[-i(\delta\varphi_L+\tau)], \tag{2.15c}$$

where

$$d=(A_R^2/A_L)\exp[-i(2\delta\varphi_R+\delta\varphi_L+3\tau)] +(A_L^2/A_R)\exp[i(\delta\varphi_R+2\delta\varphi_L+3\tau)]. \tag{2.15d}$$

The phase of each channel is referred to the center of the side of the needle. The leakage probabilities are the absolute squares of the amplitudes: $P_A=|a|^2$, etc. In this form, the probability amplitudes automatically satisfy the conditions $ab^*+bc^*+ca^*=0$ and $|a|^2+|b|^2+|c|^2=1$, which are necessary for conservation of electrons. Other forms can be derived which are more accurate for numerical work, such as

$$P_A=A_L^2/(A_L^2+A_R^2+P_3s/\pi), \tag{2.16a}$$

$$P_B=(P_3s/\pi)/(A_L^2+A_R^2+P_3s/\pi), \tag{2.16b}$$

$$P_C=A_R^2/(A_L^2+A_R^2+P_3s/\pi). \tag{2.16c}$$

The calculation of Chambers[17] is similar to ours, but in a different Landau gauge, and for $A=B=A_F$. He gave his results in terms of the magnetoresistance while we give the leakage probabilities which come into the magnetoresistance formula of Falicov, Pippard, and Sievert.[16]

There are several ways of calculating the effect of magnetic breakdown on the de Haas–van Alphen effect. In the thesis of one of the authors,[25] plausible boundary conditions were applied to the asymptotic solutions (2.9) and the density of states in energy calculated numerically. This density of states was fit to a simple formula derived by Pippard[11] (for a finite network consisting of a triangular orbit and three large loops), using the Landau-level position and the breakdown field as free parameters. Pippard showed that this density of states gives a q^3 amplitude factor for the de Haas–van Alphen effect. (For our purpose, q must be calculated using the value of H_0 chosen to fit the numerical density

of states.) Another method would be to use the numerically calculated leakage probability amplitudes (2.15) to replace the corresponding quantities in Pippard's network model,[11] and then Fourier analyze the calculated density of states. We shall discuss the relationship between these methods in Sec. III.

III. COMPARISON OF EXACT AND SEMICLASSICAL RESULTS

Extensive numerical calculations were carried out for a range of band parameters and magnetic field strengths (about 1.5–1000 kG). A typical result for the leakage probabilities is shown in Fig. 4.

The spacing of the probability peaks in inverse field gives the de Haas–van Alphen period P. Our results showed a very slight quantum effect, i.e., the spacing of low quantum number peaks is about 2.5% smaller than the Onsager-Lifshitz[27] value, which holds at large quantum numbers. The spacing of the peaks in energy gives the effective mass $m^*/m_0=\hbar eH/m_0c(E_{n+1}-E_n)$. In some cases, the effective masses for spin up and spin down were slightly different (to be discussed in Sec. IV), but the average value agrees with the Onsager-Lifshitz[27] rule to within 4%.

The leakage probability amplitudes from the semiclassical model are[28]

$$a=qe^{-i\Phi/3}[1-qe^{i\Phi}]/d, \tag{3.1a}$$

$$b=p^2/d, \tag{3.1b}$$

$$c=qp^2e^{i\Phi/3}/d, \tag{3.1c}$$

$$d=1-q^3e^{i\Phi}, \tag{3.1d}$$

where we use Pippard's rule, $q=|q|$, $p=i|p|$, and the phase of each channel is referred to the center of the side of the needle. The absolute squares of these expressions give the probabilities of Falicov, Pippard, and Sievert.[16] The quantity Φ is the phase change in one circuit of the needle orbit $\Phi=2\pi[(1/PH)+\theta]$. The semiclassical probabilities are also plotted in Fig. 4, using values of P and θ to make the location of the peaks agree with the numerical calculations, but using the semiclassical expression for p and q, including the value of the breakdown field,[5–10] which, applied to this model, gives

$$H_0=(\pi/3\sqrt{3})(\hbar c/e)(\Delta/A)^2Q, \tag{3.2a}$$

$$Q=U_p^2-(A/B)\epsilon[(\epsilon-\xi)^2-1/9]/U_p. \tag{3.2b}$$

It is seen in Fig. 4 that the exact probabilities and the semiclassical probabilities are in excellent agreement, even for very small quantum numbers (large H). Thus, we agree with Chambers[17] that the semiclassical theory of magnetoresistance of Falicov, Pippard, and Sievert[16] is accurate for zinc.

[28] A. B. Pippard, Proc. Roy. Soc. (London) **A287**, 165 (1965). The formula given in the Appendix of this work differs from (3.1) due to the different reference point for the phase.

Using the correct period and phase in (3.1) instead of those calculated on the network model (the period using the network model is off by 10–20%) seems to compensate for the distortion of the orbits in the network model. However, it is striking that the semiclassical theory is so good for small quantum numbers. We did find deviations from the semiclassical theory when $H_0\gg 1/P$, but this region is not very interesting experimentally as the breakdown effects occur only in the quantum limit ($H\gtrsim 1/P$). This last condition can be understood on a geometric argument. The semiclassical expression for p is exact for pairs of hyperbolic orbits,[9,10] the breakdown field being proportional to the "area of contact" of the orbits in k space[5,29] with the same proportionality constant that relates the inverse de Haas–van Alphen period to the area of a closed orbit.[27] For the semiclassical theory to be accurate, the regions where the needle and monster approach each other must look hyperbolic, i.e., the needle cross section must be more triangular than circular. For the needle to have sharp corners, the area of contact must be much less than the area of the needle, i.e., $H_0\ll 1/P$.

We now turn to the question of the density of states and the effect of breakdown upon the de Haas–van Alphen effect. As mentioned in Sec. II, a calculation has been done[25] applying plausible boundary conditions to the asymtotic form (2.9). In this calculation, the density of states could be fit very well with Pippard's formula,[11] but with a value of breakdown field about 0.7–0.75 of the semiclassical value (3.2). One is tempted to offer this as an explanation of the fact that the Higgins and Marcus[13] value of $H_0=2.2$ kG from the de Haas–van Alphen effect is 0.81 of the value $H_0=2.7$ kG from the magnetoresistance experiment.[1,16] However, the question of the proper boundary conditions is quite subtle and those used could be wrong. Another approach is to check the basic network model. Our numerical calculations of the phases of the leakage probability amplitudes (2.15) agree fairly closely with the phases of the semiclassical expressions (3.1). Over a range of different fields, Fermi energies, and other band parameters, we find the numerical phases are about 0.06 rad larger than the semiclassical phases. The standard deviation of about 0.03 rad is probably the error in the phase calculation, which is less accurate than the probability amplitude calculation. Thus, the Pippard network theory should be accurate for calculating the density of states, which requires the phases as well as the magnitudes of the probability amplitudes. Pippard's numerical calculations[11] gave a de Haas–van Alphen amplitude factor of q^3 for a large needle size and a factor of $q^{3.6}$ for the size appropriate to magnesium. In zinc, the needle diameter is about 20 times smaller than in magnesium, so one would expect an even larger exponent than 3.6. A factor $q^{3.6}$ (with q calculated from the semiclassical H_0) corresponds to a

[29] W. G. Chambers, Phys. Rev. **149**, 493 (1966).

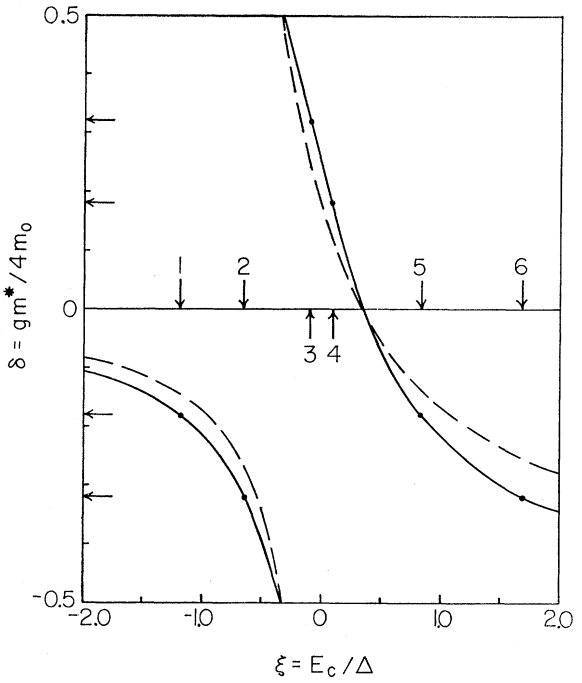

FIG. 5. The spin-splitting parameter versus the ratio of the crystal potential gap to the spin-orbit constant. The solid curve is the exact result for $B/A=1.0$ and $\epsilon\equiv\mu/\Delta=1.4$. The broken curve is the corrected Bennett-Falicov result (Ref. 3) for $B/A=1.0$. For B/A not unity, the exact curve is shifted in ξ by approximately $2.5\,\epsilon(1-B/A)$, and the right branch of the Bennett-Falicov curve is changed. However, the endpoints of the right branch are independent of B/A. The arrows on the ordinate indicate the values of δ allowed by experiment, and the arrows on the abscissa indicate the corresponding allowed values of ξ.

smaller de Haas–van Alphen amplitude, which corresponds to a smaller effective H_0 if the amplitude is represented by q^3 (as it is in both the analysis of Higgins and Marcus and in our numerical calculations).

However, the Green's-function theory of Falicov and Stachowiak[12] gives an amplitude factor q^3, with q being calculated with the semiclassical H_0. Also, Chambers obtained the same result in an approximate calculation.[29] Falicov and Stachowiak demonstrated the agreement of their method with Pippard's by a numerical calculation involving a set of orbits which did not include the needle orbit. Thus, the theoretical situation is unclear, though the two experimental breakdown fields do differ by what seems to be more than experimental error. It is important for the Pippard network model to be solved accurately for very small needle size, which limit may simplify the calculation. Because of this uncertainty, all our results for the band parameters use the magnetoresistance breakdown field.

Up to this point, the Onsager-Lifshitz[27] rules plus Pippard's semiclassical-network theory have proved adequate. However, this is not true for the spin splitting. The peaks in probability (or density of states) may be represented by $1/H=(n+\gamma+\sigma\delta)P$, where δ represents the spin splitting and is related to the g factor by $g=4\delta m_0/m^*$. The Bennett-Falicov calculation of δ uses perturbation theory and is valid if the Fermi level is very near the needle band edge, which implies that the needle cross section is circular. Their corrected result is

$$\delta=1/6\xi, \quad \xi<-\tfrac{1}{3}, \tag{3.3a}$$

$$\delta=\tfrac{1}{2}[(B/A)^2-3\xi]/[(B/A)^2+2+3\xi], \quad \xi>-\tfrac{1}{3}. \tag{3.3b}$$

Note that their result is independent of the Fermi energy and is independent of B/A for $\xi\leqslant-\frac{1}{3}$. Their result is shown in Fig. 5, for $B=A$. We calculated δ by measuring the distance between spin-up and spin-down peaks in the numerical results, such as shown in Fig. 4. The numerical result for δ is also plotted in Fig. 5 for $B=A$ and a particular Fermi level. There is an ambiguity in determining δ by our method, the same ambiguity as in analyzing the experimental results[1]: Which peaks are to be regarded as a spin-split pair? For a particular γ, we can get the same set of peak positions by changing δ by any integer; or, we can also get the same set by adding $\frac{1}{2}$ to γ and subtracting $\frac{1}{2}$ plus any integer from δ. The experimental ambiguity is twice as great, as it is not known which peaks are spin up and which are spin down. In Fig. 5, we have resolved the ambiguity in such a way as to obtain the best comparison with Bennett and Falicov.[3] Our results depend upon the Fermi energy; they agree well with Bennett and Falicov at small Fermi levels, but differ by as much as 0.1 for parameters characteristic of zinc. For B/A not equal to unity, the exact curve is shifted in ξ, whereas only the right-hand branch of the Bennett-Falicov curve is modified. Even though the agreement between the two theories seems fair for the case shown in Fig. 5, the derivatives of δ with respect to ξ and ϵ are quite different. These derivatives are needed in Sec. IV in explaining the effects of pressure. The WKB result[25] agrees well with the exact result far from the discontinuity near $\xi=\frac{1}{3}$. Instead of showing the discontinuity, the WKB result has the form of a dispersion curve.

One may still ask: "What is the true g factor?" There are several ways to answer the question which, due to the complexity of the level structure, give different answers. One method is to let the spin-orbit constant Δ approach zero so that the levels which come together can be called spin-split pairs. This works for $\xi<-\frac{1}{3}$, for the band edge stays a nondegenerate K_7 throughout the limiting process, and one finds the result shown in Fig. 5. However, for $\xi>0$, the curve of Fig. 5 would have to be shifted up by $\frac{1}{2}$ so that δ would go to zero as Δ goes to zero ($\xi\to\infty$). For the region $-\frac{1}{3}<\xi<0$, the band edge changes from K_8 to K_7 during the limiting process and the levels cannot be traced. Another method is to calculate the result if an electron-spin resonance experiment could be performed. This has been studied by using a simple model in which the K_9 level is far enough below the K_7 and K_8 levels so that it can be eliminated by perturbation theory.[25] The

result gives the same curve as in Fig. 5, except that near the discontinuity two resonances could be seen, the weaker resonance corresponding to extrapolations of each branch of the curve. Finally, one could follow Stark's suggestion[1] to see if any of the predicted levels at low quantum number are missing. In our calculations near $\xi=-\frac{1}{3}$, all the predicted levels appear (shifted somewhat by the quantum effects), though the last two peaks are so weak that they probably could not be seen experimentally. The Stark criteria would shift the left-hand branch in Fig. 5 up by $\frac{1}{2}$, and the right-hand branch down by $\frac{1}{2}$, to remove the discontinuity. However, the Stark criteria fails in this case as it is possible that there are Landau levels which move *below* the needle band edge as H increases.[2] Because of its agreement with both the dominant spin resonance and the Bennett-Falicov theory, we adopt the convention of Fig. 5, but keep in mind the possibility of ambiguity for $\xi>-\frac{1}{3}$.

IV. ENERGY-BAND PARAMETERS AND EFFECT OF PRESSURE

Our energy-band model has five parameters: E_c, Δ, A, B, and ζ. The experiments on pure zinc at atmospheric pressure give us five numbers: the de Haas–van Alphen period[30] $P=6.3\times10^{-5}$ G^{-1}, the effective mass[19,30] $m^*/m_0=0.0075$, the breakdown field[16] $H_0=2.7$ kG, and the spin-splitting parameters[1,2] $\delta=\pm0.18$, $\gamma=0.32$ (or $\delta=\pm0.32$, $\gamma=0.8$). However, the quantity γ is of limited usefulness in determining the band parameters, so we begin by fixing B/A and using the first four experimental quantities to determine the other band parameters. As was mentioned above, $B/A=1$ for nearly free electrons. A crude tight-binding calculation yielded an upper limit of $B/A=2$, so that we investigated the range 0.5–2.0. Because of the ambiguity, there are six possible solutions for δ, as indicated in Fig. 5. We number these solutions from left to right in ξ, and they correspond to $\delta=-0.18$, -0.36, 0.36, 0.18, -0.18, and -0.36, respectively.

The procedure used to find the band parameters was as follows: Values of ξ and ϵ were assumed and the WKB results for P and m^* used to fix A and Δ (unique analytic solutions exist[25]). Then for each spin the leakage probabilities were calculated for six values of H spread over a cycle near $H=H_0$, and the results for P_B least-square fitted to the semiclassical expression with H_0 and θ as adjustable parameters. The fits were quite good and H_0 was always near the semiclassical value. The difference between the θ's for spin up and spin down then provided δ. The computer then adjusted ξ and ϵ to obtain the experimental values of H_0 and δ. A large enough region of the ξ, ϵ plane was explored to make certain that there were no undiscovered solutions with reasonable parameter values. For a fixed B/A, the uncertainties in the parameters due to uncertainties in the experimental quantities were small (greatest uncertainty is 5%).

For each value of δ, the experiment requires a definite value of γ. The theoretical values of γ for cases 2, 3, and 6 agree with the experimental values to within 0.02 for the entire range of B/A while the γ values for the other cases disagree by about 0.4 or 0.5. Thus, using the value of γ reduces the number of cases by half, but does not help determine B/A. The band parameters for cases 2 and 3 are in a reasonable range compared to the previous theoretical estimates, but the spin-orbit splitting for case 6 is more than an order of magnitude smaller than the theoretical estimates.

In order to determine B/A, we make use of the experiments on the change in de Haas–van Alphen effect with pressure.[2,19,20] Three new experimental numbers are available, the change with pressure of the period, mass, and spin splitting. We now argue that only two new parameters are necessary to explain the pressure effects. First of all, hydrostatic pressure does not change the symmetry of the lattice, so that the band model (with altered values of the parameters) is valid for zinc under pressure. For an applied pressure of 1 kbar the fractional reduction in c spacing[31] is 12.23×10^{-4} and that in the a spacing is 1.55×10^{-4}. The fractional changes in the band parameters are expected to be of the same order of magnitude except in two cases. The change in the axial ratio c/a causes a large fractional change in the local Fermi energy, as has already been pointed out.[21,32,33] The free-electron Fermi energy of unstressed zinc is 0.701 Ry, while the energy of corner K is 0.697 Ry. Therefore, the local Fermi energy in the nearly free-electron approximation is the small difference of these two large numbers, 0.004 Ry. Under pressure, the two large quantities change differently; the energy at the corner is proportional to a^{-2}, while the Fermi energy is proportional to $a^{-4/3}c^{-2/3}$. The free-electron prediction for the change in local Fermi energy is $F_0\equiv d\mu/dp=0.5$ mRy/kbar. The rate of change of the crystal potential splitting E_c is also magnified. This quantity is related to the pseudopotential[6] by $E_c=\frac{3}{2}W(q)$. The value[33] of W for $q=0$ is about -0.5 Ry; but for $q=K_{100}$, which gives the energy gap at the corner, W is very nearly zero. Thus, a small change in lattice constants can give a large fractional change in E_c. The calculation of O'Sullivan and Schirber[19] using Harrison's point-ion model[34] gives $G_0\equiv dE_c/dp=0.22$ mRy/kbar. The other quantities in the band model should change very little with pressure. The velocity operators do not depend upon the lattice, so that the changes in A and B are solely due to changes

[30] A. S. Joseph and W. L. Gordon, Phys. Rev. **126**, 489 (1962).

[31] G. A. Alers and J. R. Neighbors, J. Phys. Chem. Solids **7**, 58 (1958).

[32] T. G. Berlincourt and M. C. Steele, Phys. Rev. **95**, 1421 (1954).

[33] W. A. Harrison, Phys. Rev. **131**, 2433 (1963).

[34] W. A. Harrison, Phys. Rev. **118**, 1190 (1960).

TABLE I. Energy-band parameters and predicted values of experimental quantities for the needle in zinc.

Needle band-edge symmetry type	Case 2 K_7	Case 3 K_8	Previous theory
B/A	1.15±0.05	0.7 ±0.1	0.78[a]
10^3 E_c (Ry)	−2.3 ±0.4	3.0 ±1.3	3.5[b]
10^3 Δ (Ry)	2.1 ±0.1	2.2 ±0.1	7.5[b]
10^3 μ (Ry)	2.7 ±0.1	2.6 ±0.2	1.0[b]
$(2A^2+B^2)^{1/2}/3^{1/2}A_F$	0.82±0.02	0.83±0.03	0.89[a]
10^3 F Ry/kbar	0.50±0.14	0.47±0.08	0.50[c]
10^3 G Ry/kbar	0.07±0.09	0.22±0.22	0.22[d]
$d\ \ln H_0/dp$ kbar^{-1}	−0.18±0.03	0.04±0.02	
band edge $10^4 m^*/m_0$	24 ±4	28 ±5	

[a] Ruvalds, Ref. 35.
[b] Stark and Falicov, Ref. 18.
[c] Nearly free-electron value.
[d] O'Sullivan and Schirber, Ref. 19.

in the wave functions. As the symmetry of a given state is not changed, the wave function can only be changed by mixing in other states of the same symmetry, which differ in energy by at least[23] 0.4 Ry. The form of the spin-orbit energy operator does depend upon the lattice, but most of the contribution comes from near the ions, where the potential is not changed very much by the deformation. Thus, we expect the fractional changes in A, B, and Δ to be about the same as the fractional change in lattice constant $\approx 10^{-3}$/kbar, whereas the fractional changes in μ and E_c estimated above are about 10^{-1}/kbar.

Therefore, we add the two free parameters $F \equiv d\mu/dp$ and $G \equiv dE_c/dp$ to the model, neglecting the change with pressure of the other parameters. We also add the experimental results[2,19]

$$d\ \ln P/dp = -0.32 \pm 0.015 \text{ kbar}^{-1},$$

$$d\ \ln m^*/dp = 0.14 \pm 0.02 \text{ kbar}^{-1},$$

and

$$d\ \ln|\delta|/dp = -0.16 \pm 0.08 \text{ kbar}^{-1}.$$

In the last quantity, one always takes the smallest value for $|\delta|$ (≈ 0.18). The system now contains seven parameters and seven experimental numbers (not counting γ), so that unique solutions are possible. The procedure was as follows: The calculations which determined the band parameters at a fixed B/A also provided numerical derivatives of the quantities P, m^*, H_0, and δ with respect to E_c and μ. For each B/A, values of F and G were chosen so that the experimental values of $d\ \ln P/dp$ and $d\ \ln|\delta|/dp$ were reproduced, and the predicted value of $d\ \ln m^*/dp$ calculated. Finally, B/A was varied until the calculated and experimental values of $d\ \ln m^*/dp$ agreed. The experimental errors in the pressure devivatives allow solutions for a range of B/A values.

The initial results were that solutions exist for case 2 in the B/A range of 0.9–1.2 and for case 3 in the B/A range of 0.7–1.1, and no solution exists for case 6 in the B/A range studied. However, our calculated δ-versus-pressure curve is practically linear, while the experimental results show considerable curvature. It is possible to keep the two curves in agreement within experimental error in the range 0–1.5 kbar by choosing $d\ \ln|\delta|/dp = -0.32 \pm 0.06$. With this choice, the allowed B/A range for case 2 is 0.8–1.4 and that for case 3 is 0.6–1.2.

We can narrow the range of solutions by making use of another experimental observation of O'Sullivan and Schirber.[2] They observed that the effective masses for spin up and spin down were not equal. They found that the higher-energy member of a close pair has an effective mass at least 4% smaller than that of the lower-energy member. The magnitude of our calculated fractional mass difference is about $0.4[(B/A)-1]$, with the signs being such that the results require $B/A > 1.1$ for case 2 and $B/A < 0.9$ for case 3. This reduces the size of the B/A range for each solution to 0.3 and is the best that can be done using present experimental data.

Most of the band parameters are consistent with theoretical estimates throughout the B/A range allowed by the experimental results. However, the parameter G changes sign in the allowed range for each case. Thus, we narrow the allowed range a bit by requiring that the value of G be within 50% of the theoretical estimate. The results are listed in Table I. Almost all the uncertainty in the band parameters comes from the experimental uncertainty in the pressure experiments. It is important to note that there is an experimental way of deciding which of the two cases is correct. We have calculated the pressure dependence of the breakdown field, which is different for the two cases. It is important that this difficult experimental measurement be made.

The parameters listed in Table I agree fairly well with the previous theoretical estimates, which are also listed in the table. As mentioned before, the nearly-free-electron approximation gives $B/A = 1.0$, and this is the value used by Chambers.[17] Ruvald's[35] theoretical value is in good agreement with our case 3. Both values of E_c have reasonable magnitudes, but the value for case 3 agrees well in sign and magnitude with Stark and Falicov.[18] Chambers found −1.9 and −1.5 mRy for E_c. Both cases yield the same value for the spin-orbit splitting Δ, and the value is less than a third of the value found by Stark and Falicov.[18] We could obtain their value by fitting only the zero-pressure data and choosing $B/A > 2$. This choice would require $E_c < -0.01$ Ry which is in even worse agreement with Stark and Falicov.[18] The disagreement for Δ is the most serious one, and may be because Stark and Falicov treat the entire Brillouin zone with a fairly simple model while we treat the needle alone to high accuracy. Chambers[17] found 1.2 and 2.2 mRy for Δ. The Fermi levels are the same for the two cases, and

[35] J. Ruvalds (private communication).

about 50% larger than the value which the parabolic model would give for the same period and effective mass $\mu=1.8$ mRy. The difference is a measure of the nonparabolicity of the needle, which also causes the effective mass at the bottom of the band to be about one-third of its value at the Fermi level. The quantity $(2A^2+B^2)^{1/2}/3^{1/2}A_F$ is a measure of the strength of the velocity matrix elements. It is the same in both cases, and is a little less than Ruvald's theoretical value.[35] An effect which has not been included in the band model, but which could reduce A and B, is the phonon-mediated interaction between electrons.[36] If the energies we are considering were very small compared to the Debye energy, the effect of the phonon interaction would be simply to reduce A and B. However, the Debye energy in zinc is only[37] 1.6 mRy so that the phonon interaction could introduce changes in the energy-band structure on the scale of the model we use.

The rate of change of the Fermi energy with pressure is in good agreement with the free-electron estimate for both cases. Actually, we should compare the free-electron value with the rate of change in the Fermi energy measured from the average energy of the three levels $2E_c/3$. In that case, the rates of change are $F'=0.45$ mRy/kbar for case 2 and $F'=0.54$ mRy/kbar for case 3, the corrections being smaller than the error range. As mentioned above, we reduced the range of B/A to keep the value of G near the previous theoretical estimate, but it is important to note that G did agree with the theory in part of the allowed B/A range. Also, as remarked above, the predicted change in breakdown field is different for the two cases. If we do not use the condition on G to narrow the B/A range, the uncertainties are larger but the predictions for the change of breakdown field with pressure are still distinct. However, if we do not use the difference in spin-up and spin-down masses, the ranges of the predicted $d\ln H_0/dp$ overlap somewhat. Not included in the table is the calculated pressure variation of γ, which is less than 0.01 in 1.5 kbar, in agreement with experiment.[2]

Reviewing the above discussion, we see that both cases agree for all the band parameters except B/A and E_c, for which case 3 agrees with previous theory. Thus, case 3 is for theoretical reasons the most likely of the two cases allowed by experiment.

Note that case 2 corresponds to a g factor of -170 and case 3 to $+170$ using our adopted convention. This agrees with the conclusion of O'Sullivan and Schirber,[2] even though their simple model for the Landau levels does not agree with our results. Both of the cases are in the region where the WKB result for δ is unreliable.

Figures 2 and 3 are calculated for case 2. For case 3, Fig. 2 would look roughly the same, except that the K_7 level lies below the K_9 level by about 50% more than the K_8-K_9 splitting. The Fermi-surface cross section for case 3 is very close to that in Fig. 3, which is quite triangular. Although Fig. 4 is calculated for case 3, the same curve for case 2 is almost identical, as a function of $1/H$, but with spin up and spin down interchanged.

We have extended our calculations of the de Haas–van Alphen period to 16 kbar, assuming that μ and E_c are strictly linear with pressure. Our results can be approximately described by $1/P=(1+0.32p+0.018p^2)/P_0$, where the units of p are kbar. They agree well with the measurements of O'Sullivan and Schirber,[19] up to 5 kbar, but predict a change in period at 16 kbar which is 50% larger than that observed by Itskevich *et al.*[20]

V. EFFECT OF ALLOYING

Higgins and Marcus have measured the change of the de Haas–van Alphen period,[21] mass,[21] and breakdown field[13] produced by alloying zinc with copper and aluminum. They concluded that the results could not be explained by changing the Fermi energy and band gap in a simple model. Of course, it is well known that alloying destroys the periodic symmetry of the lattice so that the band model for pure zinc should not apply. However, it is still interesting to see whether or not the data could be accounted for by distorting the pure zinc band model, especially because of the magnifying effect of the change in axial ratio c/a. Accordingly, we make the same type of model as for the change with pressure, where F and G now give the changes with concentration of solute x. The quantities A, B, and Δ are expected to have fractional changes of the order of x, while the changes in μ and E_c are magnified by the change in axial ratio (E_c is also changed by the fact that the pseudopotential for the solute can be quite different than that for zinc). The pure-zinc band parameters are now known, so we need determine only the two parameters F and G. We make this determination using the changes in period and mass, and then predict the change in the breakdown field. The experimental data for copper are $d\ln P/dx=-140\pm20$, $d\ln m^*/dx=0\pm50$, and $d\ln H_0/dx=700$. The solution for case 2 is $F=0.40$ to 0.24 Ry, $G=1.3$ to 2.2 Ry, and $d\ln H_0/dx=-300$ to -2300; while for case 3 we find $F=0.26$ to 0.62 Ry, $G=-0.04$ to -1.8 Ry, and $d\ln H_0/dx=18$ to 140. The free-electron estimate for F' (the change of Fermi level measured from $2E_c/3$) is 0.28 Ry compared with -0.5–0.1 Ry for case 2 and 0.25–0.02 Ry for case 3. A rough estimate of G can be made assuming that $W(q)$ for copper[34] is -0.2 Ry, yielding a value of -0.3 Ry for G. We see that the case 3 results for F' and G are in reasonable agreement with the simple estimates, but that neither case can account for the experimental change in the breakdown field. For the aluminum alloys, neither the period nor the mass changes within experimental error, so that F and G are small. How-

[36] See, for example, S. Engelsberg and J. R. Schrieffer, Phys. Rev. **131**, 993 (1963); P. B. Allen, M. L. Cohen, L. M. Falicov, and R. V. Kasowski, Phys. Rev. Letters **21**, 1794 (1968).

[37] G. Borgonovi, G. Caglioti, and J. J. Antal, Phys. Rev. **132**, 683 (1963).

ever, the experimental result is $d\ln H_0/dx=2400$, so the distorted band model cannot explain the effect of alloying upon breakdown, in agreement with the conclusion of Higgins and Marcus.[13]

Lawson and Gordon[22] have measured the de Haas–van Alphen periods and masses as a function of temperature for alloys with cadmium and mercury, which have the same number of valence electrons per atom as pure zinc. They found that their results and those for pure zinc under pressure fall on the same curve of period-versus-axial ratio c/a, and that $d\ln P/d(c/a)=120\pm11$. They also find that the mass change is given by $d\ln m^*/d(c/a)=-100\pm25$. Redefining F and G to give the changes in μ and E_c with respect to c/a, we find for case 2, $F=0.1\pm0.2$ Ry and $G=0.9\pm0.5$ Ry, and for case 3, $F=0.0\pm0.2$ Ry and $G=-0.9\pm0.5$ Ry. The F' values from our results are -0.4 ± 0.1 Ry for case 2 and -0.3 ± 0.1 Ry for case 3, both being in reasonable agreement with the nearly-free-electron value, $F'=-0.26$ Ry. Note that the change in the crystal potential gap is much larger than the change in the Fermi energy. Both case 2 and case 3 predict that the K_7 and K_8 levels cross at $c/a=1.833\pm0.002$ and that the needle disappears at $c/a=1.836\pm0.003$. The c/a value for pure zinc[22] is 1.830. The lower end of the prediction for disappearance of the needle is inconsistent with Lawson and Gordon's observation of de Haas–van Alphen oscillations for c/a ratios as large as 1.836. Thus, our estimate is that the needle disappears at about $c/a=1.838\pm0.001$, in good agreement with a linear extrapolation of the data. This c/a value is also near the maximum of steady diamagnetism found by Lawson and Gordon.

VI. SUMMARY AND CONCLUSIONS

Our numerical calculations show that the network theory of Pippard,[7,11] using the semiclassical breakdown probability, corrected by the Onsager-Lifshitz[27] rules for the spacing of Landau levels, and given the correct de Haas–van Alphen phase factors, yields good results for all the features of the Landau levels. The probabilities calculated by Falicov, Pippard, and Sievert[16] and used by them to explain the magnetoresistance experiments are accurate, a conclusion in agreement with Chambers.[17] Solution of the network model for the density of states and then carrying out a Fourier analysis should yield the effect of breakdown upon the de Haas–van Alphen effect, but it is not at present clear if this calculation would yield the result of Falicov and Stachowiak.[12]

The Bennett-Falicov[3] theory of the g factor is accurate only if the Fermi level is near the needle band edge. The simple WKB theory of the g factor[25] is accurate far from the discontinuity which, occurs at $E_c\approx-(\Delta/3)+2.5\mu(1-B/A)$. Because of the dependence on B/A, it is not yet possible to say whether the WKB theory is valid for the other hexagonal metals.

Using the experimental data from the de Haas–van Alphen effect and its change with pressure, two possible sets of band parameters have been found which are allowed experimentally. Agreement with previous theory selects case 3, but an experimental way of choosing would be provided by a measurement of the change in breakdown field with pressure.

The principle effect of pressure upon the band structure is to change the local Fermi energy and the crystal potential gap. Changes of these quantities agreeing with simple theoretical estimates explain the pressure dependence of the de Haas–van Alphen effect.

The changes in de Haas–van Alphen period and effective mass due to alloying by Cu, Al, Cd, and Hg can be accounted for by changing the local Fermi energy and the crystal potential gap by amounts which agree with simple theoretical estimates. However, the predicted change in breakdown field is in strong disagreement with the experiment, which is the same conclusion reached by Higgins and Marcus.[13]

Note added in proof. The rate of change of E_c with respect to c/a from band theory[18] is approximately $G=-1$ mRy, in good agreement with case 3.

ACKNOWLEDGMENTS

The authors wish to thank Professor L. M. Falicov, Professor W. L. Gordon, Professor W. A. Harrison, Professor R. J. Higgins, Professor J. Ruvalds, and Professor W. J. O'Sullivan for very interesting and helpful conversations during this work. We also wish to thank Professor Falicov, Professor Ruvalds, Professor Gordon, and Dr. J. R. Lawson for communicating their results prior to publication.